https://doi.org/10.37434/tpwj2022.01.09

METHODS AND MEANS OF EARLY VIBRATION DIAGNOSTICS OF ROTATING COMPONENTS OF MECHANISMS OF QUAY CONTAINER HANDLERS

I.M. Javorskyi[1,2], R.M. Yuzefovych[1,3], O.V. Lychak[1], P.O. Semenov[4]

[1]Karpenko Physico-Mechanical Institute of the NASU
5 Naukova Str., 79060, Lviv, Ukraine,
[2]Politechnika Bydgoska
7 Prof. Sylwestra Kaliskiego, 85796, Bydgoszcz, Poland,
[3]Lviv Polytechnic National University
12 Stepan Bandera Str., 79013 Lviv, Ukraine,
[4]Odesa National Maritime University
34 I. Mechnikov Str., 65029, Odesa, Ukraine

ABSTRACT

The paper describes the properties of a model of vibration of interconnected rotating mechanisms in the form of biperiodically nonstationary random processes (BPNRP). Individual cases of such a model are considered, which enable performing data analysis by the method of periodically nonstationary random processes (PNRP). These methods are used to analyze the condition of mechanisms at increased vibration level. Separation of deterministic and stochastic vibrations was performed and parameters describing the structure of hidden periodicities of the first and second order were determined. The causes for increased vibration level were established.

KEY WORDS: lifting mechanism, vibration, periodical nonstationarity, deterministic oscillations, amplitude spectrum, stochastic high-frequency modulation, dispersion

INTRODUCTION

In vibration diagnostic systems the carriers of information on the technical condition of a mechanism are displacement, speed or acceleration of contact surfaces of the mechanisms, arising as a result of their defective part interaction. The nature of such an interaction is reflected in the parameters of the recorded vibration signals. In order to fulfill the description and analysis of the regularities of the latter, it is necessary to substantiate their adequate mathematical models, methods and algorithms of processing and computer support of the processes of extraction of the diagnostic features and taking decisions on the technical condition of the diagnosed object.

Vibration signals of rotating mechanisms are characterized by rhythmic variability, the main features of which are cyclic repeatability and stohasticity. Nonlinear effects, arising in mechanical systems at appearance of defects, lead to their interaction, which is reflected in the signal properties in the form of modulations. Such a modulation is quantitatively characterized by parameters, describing the structure of periodical or almost periodical time changes of moment functions of the first and second orders of the respective classes of nonstationary random processes [1–11]. It is rational to use these parameters at formation of diagnostic features to reveal the defects. As shown by investigations [1, 7–9, 12], application of such features enables detecting defects at early stages of their development and conducting effective monitoring of the diagnosed object.

Vibrations of mechanisms, consisting of many rotating components, have complex polyrhythmic structure. It is due, primarily, to different rotation speeds of individual elements. So, depending on the defect location, vibrations of the rolling bearing can be characterized by oscillations with shaft rotation frequencies, frequencies of rotation of the rolling bodies on the inner or outer rings, separator frequencies, as well as frequencies, determined by their combinations. Gear pair vibrations can have oscillations with shaft rotation frequencies, gear meshing frequencies and their combinations. Therefore, in the general case, vibrations can be described by polyperiodically nonstationary random processes [1, 3, 4], which belong to the class of almost periodically nonstationary processes. In the simplest case, when just two stochastic rhythms interact with each other, we come to a model in the form of a biperiodically nonstationary random process. Below we will briefly characterize such a model of vibration signal, and will consider separate cases, which allow substantiating analysis of vibrations of objects with complex kinematics, using the methods of periodically nonstationary random processes.

BPCRP MODEL OF A VIBRATION SIGNAL

The effectiveness of the methods of processing the cyclostationary signals at monitoring the machine condition can be generally explained by their ability to detect modulations, caused by appearance of malfunctions. The effects of modulation in the vibration model in the form of periodically correlated random processes (PCRP), which describe the stochastic repeatability with one period, are characterized by mutually stationary random processes in their harmonic representation [1, 11, 13]:

$$\xi(t)=\sum_{k\in\mathbb{Z}}\xi_k(t)e^{ik\frac{2\pi}{P_1}t},$$

where Z is the set of integers i; P_1 is the period of nonstationarity (period of rotation of one of the gears). Generalizing these representations, we can come to the conclusion that modulation of two stochastic periodicities which is due to rotation of the two gears can be expressed as follows:

$$\xi(t)=\sum_{k\in\mathbb{Z}}\xi_k^{(P_2)}(t)e^{ik\frac{2\pi}{P_1}t}, \quad (1)$$

where frequency harmonic $2\pi/P_1$ and its multiples are modulated by PCRP with period P_2:

$$\xi_k^{(P_2)}(t)=\sum_{l\in\mathbb{Z}}\xi_{kl}(t)e^{il\frac{2\pi}{P_2}t}.$$

Therefore, for random process (1), we have;

$$\xi(t)=\sum_{k,l\in\mathbb{Z}}\xi_{kl}(t)e^{i\Lambda_{kl}t}, \quad (2)$$

where $\xi_{kl}(t)$ are the mutually stationary random processes and $\Lambda_{kl}=k\left(\frac{2\pi}{P_1}\right)+l\left(\frac{2\pi}{P_2}\right)$. Note that process (2) is the sum of amplitude- and phase-modulated harmonics, where Λ_{kj} frequencies are a linear combination of two fundamental frequencies $\Lambda 10 = k(2\pi/P_1)$ and $\Lambda_{01} = l(2\pi/P_2)$. Mathematical expectations of modulating processes $m_{kl} = E\xi_{kl}(t)$ are Fourier coefficients of the mean function:

$$m(t)=E\xi(t)=\sum_{k,l\in Z}m_{kl}e^{i\Lambda_{kl}t}. \quad (3)$$

For correlation function $R(t,\tau)=E\overset{\circ}{\xi}(t)\overset{\circ}{\xi}(t+\tau)$, $\overset{\circ}{\xi}(t)=\xi(t)-m(t)$ we have:

$$R(t,\tau)=\sum_{k,l\in Z}R_{kl}(\tau)e^{i\Lambda_{kl}t}, \quad (4)$$

where

$$R_{kl}(\tau)=\sum_{p,q\in Z}r_{p-k,q-l,p,q}e^{i\Lambda_{pq}\tau}, \quad (5)$$

and $r_{pqkl}(\tau)=E\overline{\overset{\circ}{\xi}_{pq}(t)}\overset{\circ}{\xi}_{kl}(t+\tau)$, $\overset{\circ}{\xi}_{pq}(t)=\xi_{pq}(t)-m_{pq}$ are the cross-correlation functions of the modulation process, sign "–" denotes complex conjugation. Thus, Fourier coefficients of correlation function (4) are defined by cross-correlation functions of modulating processes, where the indices are shifted by k and l, respectively. It follows from (5) that mutual correlations of modulating processes $\xi_{kl}(t)$ with different indices lead to biperiodical nonstationarity of the second order. This results in correlations of the respective spectral components, which are quantitatively characterized by Fourier transformation of expression (5):

$$f_{kl}(\omega)=\frac{1}{2\pi}\int_{-\infty}^{\infty}R_{kl}(\tau)e^{-i\omega\tau}d\tau. \quad (6)$$

It follows from (5) that:

$$f_{kl}(\omega)=\sum_{p,q\in Z}f_{p-k,q-l,p,q}(\omega-\Lambda_{pq}),$$

where

$$f_{pqkl}(\omega)=\frac{1}{2\pi}\int_{-\infty}^{\infty}r_{pqkl}(\tau)e^{-i\omega\tau}d\tau$$

are the mutually spectral densities of modulating processes $\xi_{pq}(t)$. Values (5) and (6) are called the correlation and spectral components, respectively [1–3]. Zero correlation component $R_{00}(\tau)$ is defined by self-correlated function $r_{pq}(\tau)=E\overline{\overset{\circ}{\xi}_{pq}(t)}\overset{\circ}{\xi}_{pq}(t+\tau)$:

$$R_{00}(\tau)=\sum_{p,q\in Z}r_{pq}(\tau)e^{-i\Lambda_{pq}\tau}.$$

This is the time-averaged correlation function of random process (2), i.e. the correlation function of its stationary approximation.

Zero spectral component

$$f_{00}(\omega)=\sum_{p,q\in Z}f_{pq}(\omega-\Lambda_{pq}) \quad (7)$$

is the spectral density of stationary approximation power for (2). It defines the spectral decomposition of time-averaged instantaneous power of oscillations $R(0, t)$. Random processes, mathematical expectations and correlation function, which are biperiodic functions and which can be represented by series (3) and (4), are called BPCRP. Fourier coefficients of the correlation function and spectral density are the general characteristics of amplitude and phase modulation of BPCRP carrier harmonics. Zero spectral

component, as one can see from (7), is the total power of spectral densities of modulating processes $\xi_{pq}(t)$, shifted by Λ_{pq}. Spectral component $f_{kl}(\omega)$ (6) is the sum of shifted mutually spectral densities of modulating processes, where the indices differ by k and l, respectively. Proceeding from the above statements, we can conclude that $f_{00}(\omega)$ describes the oscillation spectrum, and $f_{kl}(\omega)$ functions give the correlation of this spectrum harmonics, where the frequencies are shifted by $\Lambda_{kl} = k\left(\frac{2\pi}{P_1}\right) + l\left(\frac{2\pi}{P_2}\right)$. These correlations are not equal to zero, except if the processes of modulation with the respective numbers are interrelated.

Individual cases of hidden periodicity of biorhythms are easily derived from expression (2). We will extract only those of them, which can be readily analyzed in terms of PNRP approach.

Suppose that $\xi_{kl}(t) = c_{kl} + \xi_{k0}(t) + \xi_{0l}(t)$, where c_{kl} are certain complex numbers, while $\xi_{k0}(t)$ and $\xi_{0l}(t)$ — are stationary random processes. Then:

$$\xi(t) = \sum_{k,l\in Z} c_{kl} e^{i\Lambda_{kl}t} + \sum_{k\in Z} \xi_{k0}(t) e^{ik\frac{2\pi}{P_1}t} + \\ + \sum_{l\in Z} \xi_{0l}(t) e^{ik\frac{2\pi}{P_2}t} = s(t) + \xi_1(t) + \xi_2(t). \quad (8)$$

Here, $s(t)$ is the biperiodic function. If $\{\xi_{k0}(t), k \in Z\}$ and $\{\xi_{l0}(t), l \in Z\}$ sets are uncorrelated, and random processes which belong to each of them, are stationary coupled, then $\xi_1(t)$ and $\xi_2(t)$ are PNRP. Additive model (8) can be applied to analysis of vibrations of two damaged components, where development of defects does not affect each other. In the case of a single-defect component, one of the PNRP in representation (8) becomes a stationary random process. Then, the random processes, which describe the modulations, namely $\xi_{k0}(t)$ or $\xi_{0l}(t)$, are uncorrelated.

We derive a multiplicative model in the form of the product of two PNRP with different periods P_1 and P_2 in the case, when $\xi_{kl}(t) = \xi_{k0}(t)\xi_{0l}(t)$. Then:

$$\xi(t) = \sum_{k\in Z} \xi_{k0}(t) e^{ik\frac{2\pi}{P_1}t} \sum_{l\in Z} \xi_{0l}(t) e^{il\frac{2\pi}{P_2}t} = \xi_1(t)\xi_2(t).$$

Analysis of such a model can be performed by PNRP methods, if one of the periods significantly exceeds the value of the other one. If only one of the components is defective, then actually its vibrations will be described by PNRP, and those of the other one — by a stationary random process $\eta(t)$. Then, $\xi(t) = \eta(t)\xi_1(t)$. In such a presentation, the influence of a defectfree component is reflected in the interaction of modulation characteristics of the damaged component carrier harmonics.

INVESTIGATION OF VIBRATIONS OF QUAY CONTAINER HANDLER

In September, 2021, the staff of the Department of the Methods and Means of Extraction and Processing of Diagnostic Signals of G.V. Karpenko Physico-Mechanical Institute of the NAS of Ukraine (PMI), together with the representatives of PORTTEKH-

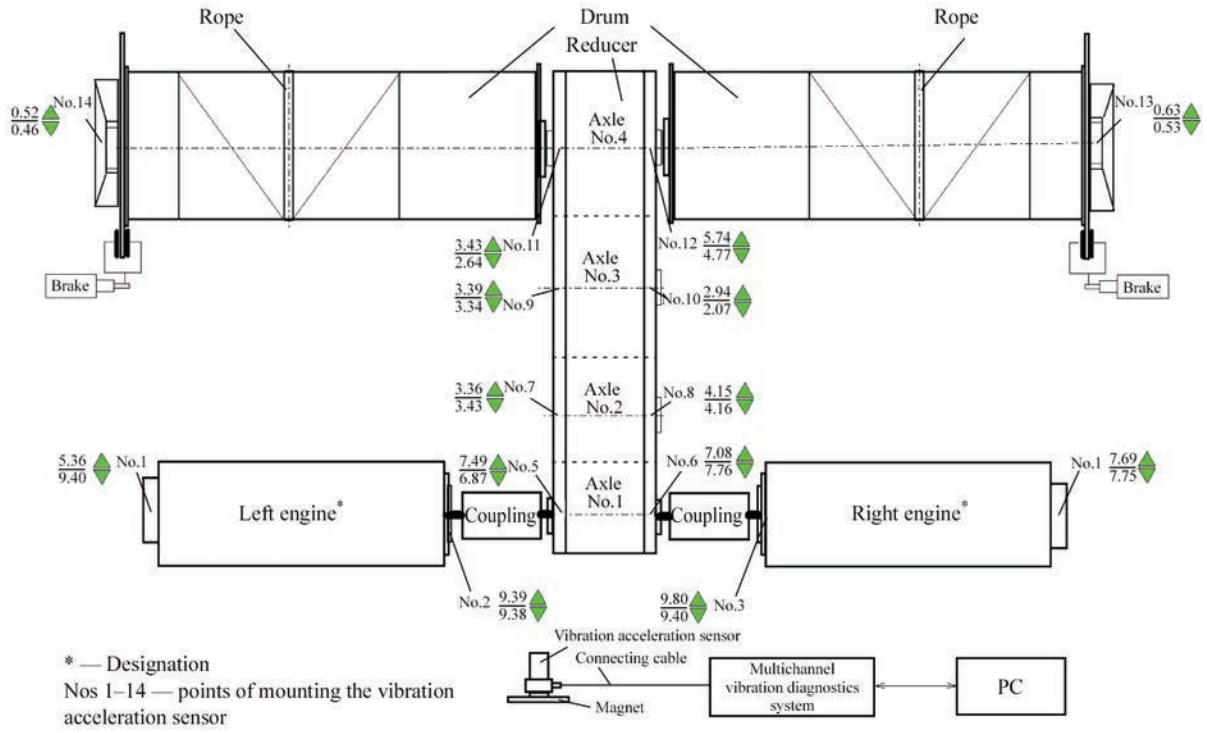

Figure 1. Scheme of arrangement of control points and measured RMS values of vibration acceleration (lifting and lowering) for Crane 1

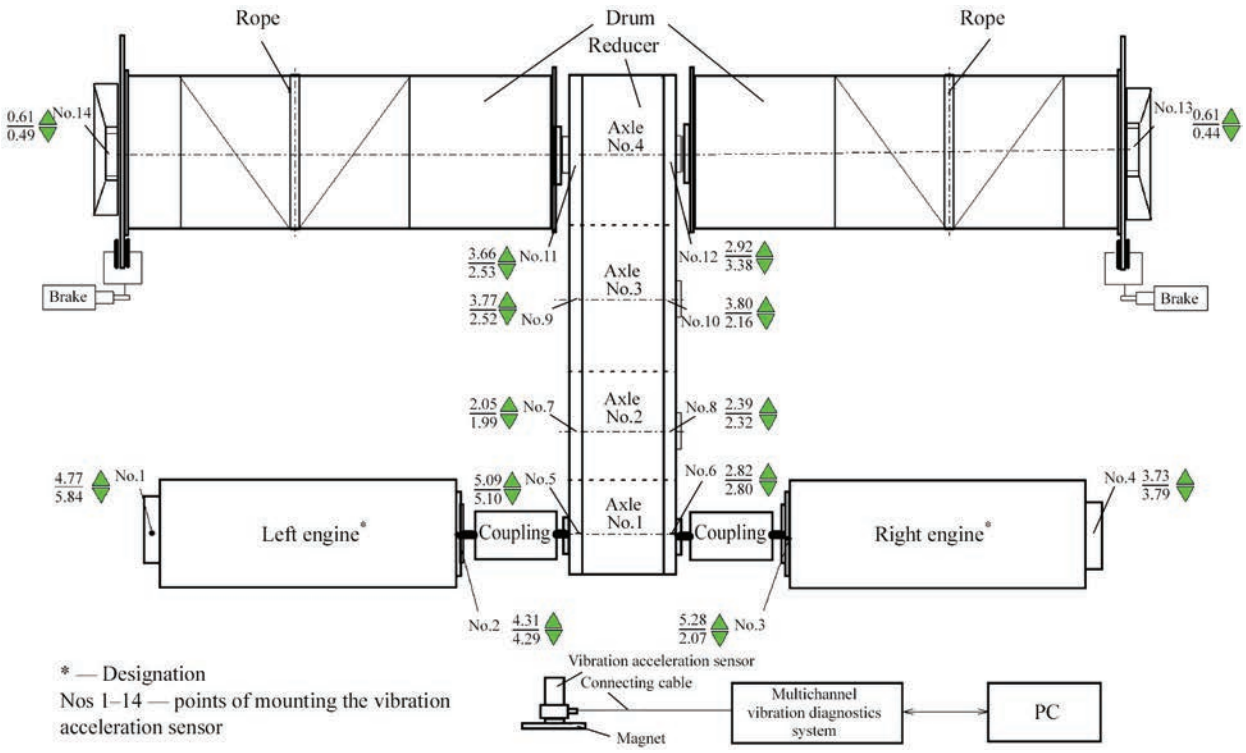

Figure 2. Scheme of arrangement of control points and measured RMS values of vibration acceleration (lifting and lowering) for Crane 2

EXPERT Company performed measurements and recording of signals of vibrations of lifting mechanism of quay container handlers ZPMC (Crane 1 and Crane 2, respectively), which belong to Brooklyn Kyiv Port Company. This Company is the operator of container terminal based on quays Nos 42, 43 of State Company "Odessa Sea Trade Port".

The layout of drive mechanism control points is given in Figures 1, 2. During performance of measurements, the sensors were fastened to the mechanism housing by magnets. Vibration acceleration was recorded in each point, and its root mean square (RMS) value was determined at crane mechanism operation for lifting and lowering of the spreader without the payload, using vibration acceleration sensors AVS-117. The sampling frequency of vibration signals was 10 kHz, the input signal frequency band was from 2 Hz to 2 kHz, and duration of recording the signal realizations for each control point was 2 s.

Determination of vibration levels of the mechanisms was conducted in keeping with DSTU ISO 10816-1:2007 "Classes of mechanisms and their vibration norms" by vibration diagnostic system COMPACT-VIBRO, which was developed at PMI [15, 16].

Table 1. Evaluation of the mechanism technical condition by vibration intensity (ISO 2372)

<table>
<tr><td colspan="2">Vibration level (RMS value)</td><td colspan="4">Mechanism classes</td></tr>
<tr><td>By vibration speed</td><td>By vibration acceleration</td><td>Small mechanisms $P < 15$ kW</td><td>Medium-sized mechanisms 15 kW $< P <$ 75 kW</td><td>Large-sized mechanisms on rigid foundations $P > 300$ kW</td><td>Large-sized mechanisms with non-rigid fastening $P > 300$ kW</td></tr>
<tr><td>mm/s</td><td>m/s^2</td><td>Class 1</td><td>Class 2</td><td>Class 3</td><td>Class 4</td></tr>
<tr><td>44.6</td><td>70.1</td><td rowspan="6">C</td><td rowspan="4">C</td><td rowspan="2">C</td><td>C</td></tr>
<tr><td>28.2</td><td>44.2</td><td rowspan="2">B</td></tr>
<tr><td>17.8</td><td>27.9</td></tr>
<tr><td>11.2</td><td>17.6</td><td rowspan="2">B</td></tr>
<tr><td>7.1</td><td>11.1</td><td rowspan="4">A</td></tr>
<tr><td>4.5</td><td>7.2</td><td rowspan="2">B</td><td rowspan="4">A</td></tr>
<tr><td>2.8</td><td>4.4</td></tr>
<tr><td>1.8</td><td>2.8</td><td rowspan="2">B</td><td rowspan="4">A</td></tr>
<tr><td>1.12</td><td>1.8</td></tr>
<tr><td>0.71</td><td>1.1</td><td rowspan="2">A</td></tr>
<tr><td>0.45</td><td>0.7</td></tr>
<tr><td colspan="6">A — satisfactory vibration value; B — admissible vibration value; C — emergency vibration value.</td></tr>
</table>

Table 2. Calculated RMS values of vibration acceleration of mechanism drive elements for Crane 1

Point number	Component description	Actual RMS value, m/s²		Boundary RMS values, m/s²
		At lifting	At lowering	
1	Left engine	5.36	9.40	11.1
2		9.39	9.38	11.1
3	Right engine	9.80	9.40	11.1
4		7.69	7.75	11.1
5	Reducer	7.49	6.87	11.1
6		7.08	7.76	11.1
7		3.36	3.43	11.1
8		4.15	4.16	11.1
9		3.39	3.34	11.1
10		2.94	2.07	11.1
11		3.43	2.64	11.1
12		5.74	4.77	11.1
13	Outrigger of the right drum	0.63	0.53	11.1
14	Outrigger of the left drum	0.52	0.46	11.1

Table 3. Calculated RMS values of vibration acceleration of mechanism drive elements for Crane 2

Point number	Component description	Actual RMS value, m/s²		Boundary RMS values, m/s²
		At lifting	At lowering	
1	Left engine	4.77	5.84	11.1
2		4.31	4.29	11.1
3	Right engine	5.28	2.07	11.1
4		3.73	3.79	11.1
5	Reducer	5.09	5.10	11.1
6		2.82	2.80	11.1
7		2.05	1.99	11.1
8		2.39	2.32	11.1
9		3.77	2.52	11.1
10		3.80	2.16	11.1
11		3.66	2.53	11.1
12		2.92	3.38	11.1
13	Outrigger of the right drum	0.61	0.44	11.1
14	Outrigger of the left drum	0.61	0.49	11.1

In keeping with DSTU ISO 10816-1:2007 the examined mechanisms belong to class 3 (powerful prime movers and other powerful mechanisms with rotating masses, mounted on massive foundations relatively rigid in the direction of vibration measurement).

Normative RMS values of vibration acceleration, which allow evaluation of the technical condition of the mechanism in keeping with the established norms of vibration intensity, are given in Table 1.

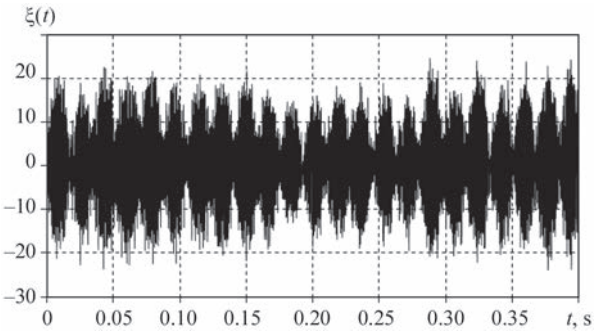

Figure 3. Signal realization segment

Evaluation of the condition of mechanism components was based on determination of RMS value of vibration accelerations (see Tables 2, 3).

As follows from Table 2, mean root square values of vibrations in bearing units of Crane 1 turned out to be higher and close to boundary values. In order to determine the causes for such a condition, the derived realizations of vibration signals were analyzed using the procedure developed by us.

ANALYSIS OF VIBRATION STRUCTURE AND DETERMINATION OF ITS PARAMETERS

The segment of realization of one of the recorded signals of vibration acceleration is shown in Figure 3. As one can see from Figure 3, vibrations have the form of clearcut groups, following each other with the frequency of approximately 60 Hz. In order to establish the general properties of the signals, in particular, their spectral composition, the correlation functions and spectral densities of their stationary approxima-

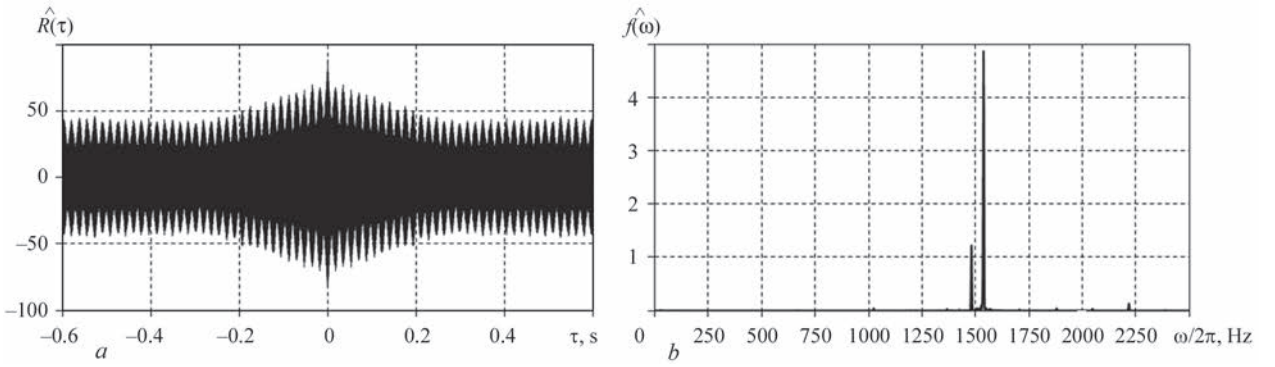

Figure 4. Evaluation of the correlation function (*a*) and spectral density (*b*)

tions were calculated. The following dependencies were used for this purpose:

$$\hat{R}(jh) = \frac{1}{K}\sum_{n=0}^{K-1}\left[\xi(nh) - \hat{m}\right]\left[\xi\left((n+j)h\right) - \hat{m}\right],$$

$$\hat{m} = \frac{1}{K}\sum_{n=0}^{K-1}\xi(nh),$$

$$\hat{f}(\omega) = \frac{h}{2\pi}\sum_{n=-L}^{L} k(nh)\hat{R}(nh)\cos\omega nh,$$

where $h = T/K$ is the discretization step; T is the time of signal recording; j is the integer number; $L = \tau_m/h$ is the natural number; τm is the point of correlogram truncation; $k(nh)$ is the correlation window. In this case, Hamming window was selected:

$$k(\tau) = \begin{cases} 0.54 + 0.46\cos\dfrac{\pi\tau}{\tau_m}, |\tau| \le \tau_m, \\ 0, |\tau| > \tau_m. \end{cases}$$

Results of calculation of one of the signals are shown in the form of graphic dependencies in Figure 4. It follows from the data of Figure 4, that group structure is preserved also in the dependence of the correlation function on the shift. Its characteristic feature also is the nonvanishing "tail", which is indicative of the presence of a deterministic component in the vibration composition. Frequency dependence of the signal spectral density shows (Figure 4, *b*) that the main part of vibration power is concentrated in the high-frequency region, the high-frequency oscillations being mostly the narrowband ones. The values of spectral density in the low-frequency region are barely noticeable against the background of powerful peaks in [1.4 kHz; 1.6 kHz] range. Therefore, for a more probable analysis of the low-frequency vibrations, we will divide the frequency region of the signals into two ranges: [0 kHz; 1.0 kHz] and [1.0 kHz; 2.5 kHz]. The graphs of evaluation of the correlation function and spectral density of the low-frequency signal component power are given in Figure 5. The spectral density is of a peaked nature, and nonvanishing oscillations of the correlation function show that this spectrum is mixed and a considerable fraction of the signal power belongs to deterministic oscillations.

Further detalization of vibration structure requires, first of all, separating their deterministic and stochastic components. The first step in such a separation is determination of the nonstationarity period (basic frequency) of deterministic oscillations. For this purpose, it is rational to use the least squares method as the most effective one [1, 17], which is reduced to searching for the coordinates of the maximum values of functional:

$$\hat{F}_1(\theta) = \frac{1}{2K+1}\sum_{n=-K}^{K}\hat{m}^2(\theta, nh), \qquad (9)$$

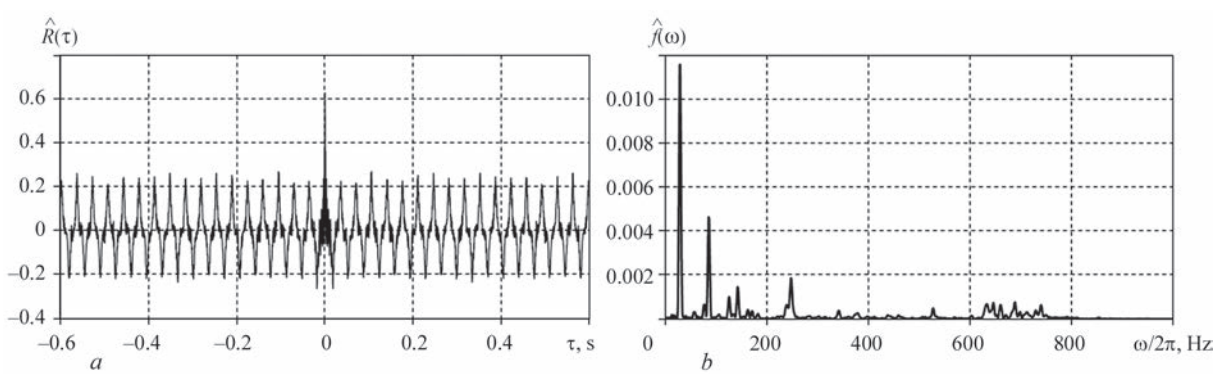

Figure 5. Evaluation of the correlation function (*a*) and spectral density (*b*) of the low-frequency signal

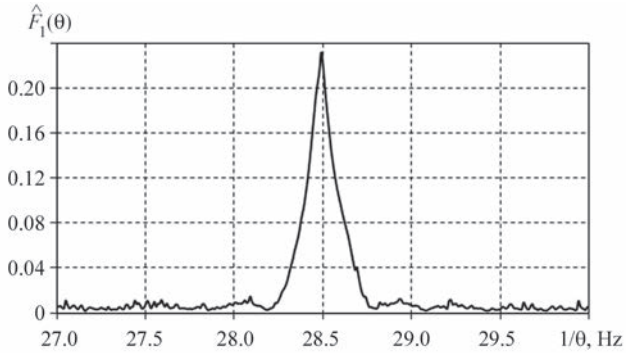

Figure 6. Quadratic functional (13), depending on trial frequency

where

$$\hat{m}(\theta, nh) = \sum_{k=1}^{L_1}\left[\hat{m}_k^c(\theta)\cos k\frac{2\pi}{\theta}nh + \hat{m}_k^s(\theta)\sin k\frac{2\pi}{\theta}nh\right],$$

$$\begin{Bmatrix}\hat{m}_k^c(\theta)\\ \hat{m}_k^s(\theta)\end{Bmatrix} = \frac{2}{2K+1}\sum_{n=-K}^{K}\xi(nh)\begin{Bmatrix}\cos k\frac{2\pi}{\theta}nh\\ \sin k\frac{2\pi}{\theta}nh\end{Bmatrix}, \quad (10)$$

while θ is the so-called "trial" period and L_1 is a certain chosen number of the harmonics. Note that the maximum value of functional (9) is close to average power of the deterministic component of oscillations.

The graph of the dependence of quadratic functional (9) on trial frequency $f = 1/\theta$ for $L_1 = 30$ is shown in Figure 6. Frequency value at which the functional value reaches its maximum was taken as the estimate of basic frequency $\hat{f}_0 = 1/\hat{P}_1$. With an accuracy of up to three digits we find $\hat{f}_0$ = 28.480 Hz. The found value corresponds to the engine rotor frequency. Total power of the rotation harmonics, which is determined by value (9) in point $\hat{f}_0$, is equal to $\hat{F}_1\left(\frac{1}{\hat{f}_0}\right) = 0.24\left(\frac{\text{m}}{\text{s}^2}\right)^2$. This value is equal to a little less than half of the total power of low-frequency oscillations, which is determined by the value of correlation function evaluation in point τ = 0, i.e. $\hat{R} = (0) = 0.62\left(\frac{\text{m}}{\text{s}^2}\right)^2$ (see Figure 5, *a*).

Substituting $\hat{f}_0$ value into formula (10) instead of 1/θ, we will calculate the cosine and sine coefficients, and proceeding from them — the amplitudes of the respective harmonics:

$$A\left(k\hat{f}_0\right) = \sqrt{\left(\hat{m}_k^c\right)^2 + \left(\hat{m}_k^s\right)^2}. \quad (11)$$

The amplitude spectrum (11) in the form of a diagram is shown in Figure 7, *b*. As we can see the spectrum is rather wide. However, the greatest part of the deterministic oscillation power belongs to the first three harmonics.

Figure 7, *a*, shows the time dependence of periodic function:

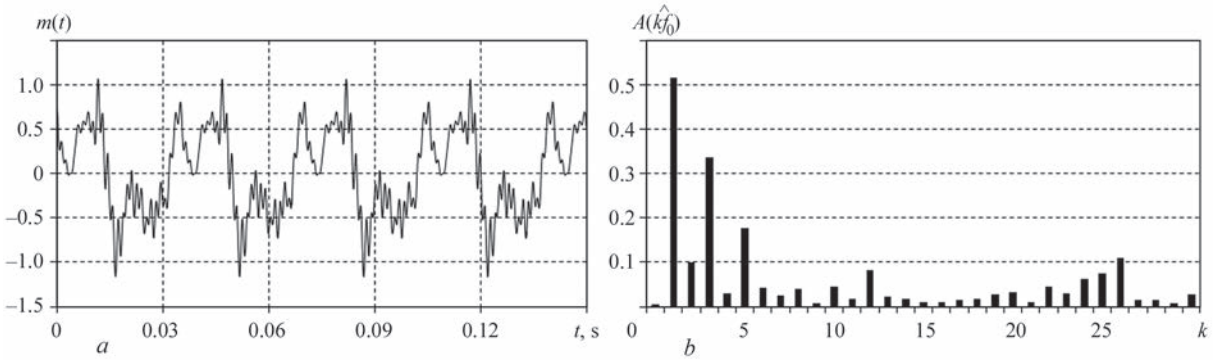

Figure 7. Deterministic oscillations (*a*) and their amplitude spectrum (*b*)

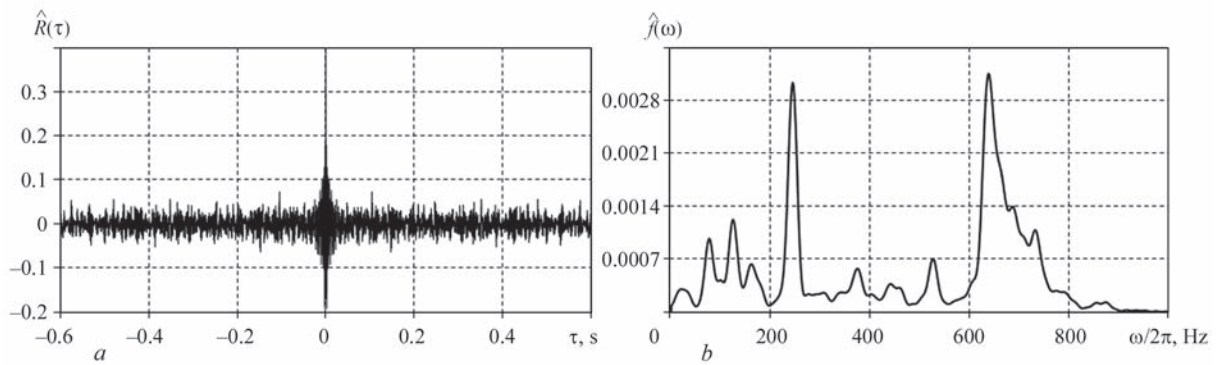

Figure 8. Evaluation of the correlation function (*a*) and spectral density (*b*) of the stochastic component of low-frequency signal

$$\hat{m}(t)=\sum_{k=1}^{30}\left[\hat{m}_k^c(\theta)\cos 2\pi k f_0 t+\hat{m}_k^s(\theta)\sin 2\pi k f_0 t\right], \quad (12)$$

which, if the following condition is satisfied:

$$h\le\frac{P_1}{2L_1+1}$$

is the interpolation formula for the deterministic vibrations, excited by rotor rotation.

Knowing dependence (12) for all $t \in [0, P_1]$, we will separate residual vibrations $\overset{\circ}{\xi}(t)=\xi(t)-\hat{m}(t)$ and will conduct their spectral-correlation analysis. The graphs of correlation function and spectral density, calculated on the base of time series $\overset{\circ}{\xi}(nh)$, are shown in Figure 8. The correlation function now vanishes quickly to the level of low-power oscillations (Figure 8, *a*). The residual spectral density, similar to the initial signal, has a ridge-like structure (Figure 8, *b*), which is due to low-power harmonics with the frequencies characteristic for the bearing, their combinations, as well as narrowband stochastic modulation of these harmonics. These low-power residual oscillations have a slight influence on the mechanism operation, so that now we can extract a deterministic periodic function in formula (8), which is presented by finite series (12).

Now we will move over to analysis of vibrations in [1.0 kHz; 2.5 kHz] range (Figure 9). Evaluation of

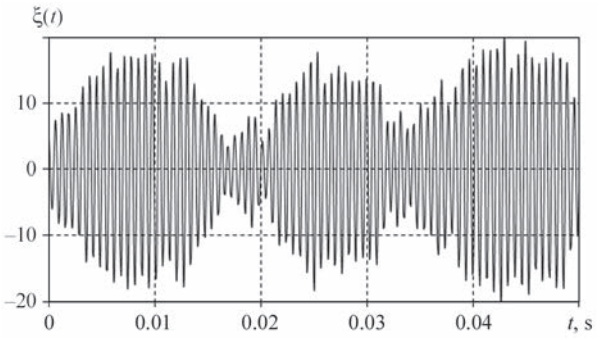

Figure 9. High-frequency signal realization segment

the correlation function at large shifts has the form of nonvanishing high-frequency oscillations (Figure 10, *a*, *b*) that can be caused by the presence of a deterministic component. In order to confirm such an assumption, we will calculate functional (9), varying the trial frequency in [1470 Hz, 1490 Hz] and [1525 Hz, 1545 Hz] ranges. Obtained clearcut peaks in the graphs of frequency dependence of functional (13) at frequencies $\hat{f}_0^1$ = = 1481.13 Hz and $\hat{f}_0^2$ = 1538.11 Hz (Figure 11, *a*, *b*) provide an affirmative answer to this. Having calculated by expressions (10) the respective harmonic amplitudes, we have $A\left(\hat{f}_0^1\right)$ = 4.163 m/s² and $A\left(\hat{f}_0^2\right)$ = 7.833 m/s². Total power of the harmonics is equal to 39.35 $(m/s^2)^2$ that is equal to approximately half of the total power of high-frequency vibrations.

We will express the high-frequency deterministic oscillations as follows:

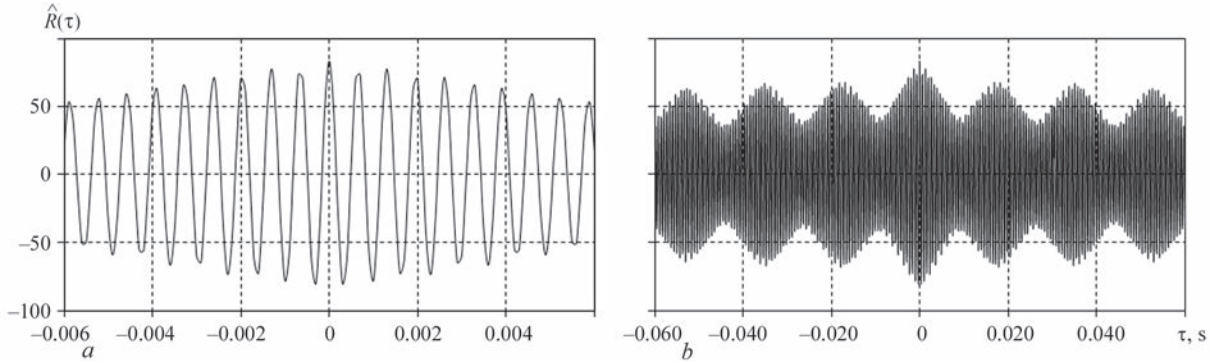

Figure 10. Evaluation of the correlation function of high-frequency signal for initial (*a*) and large (*b*) shifts

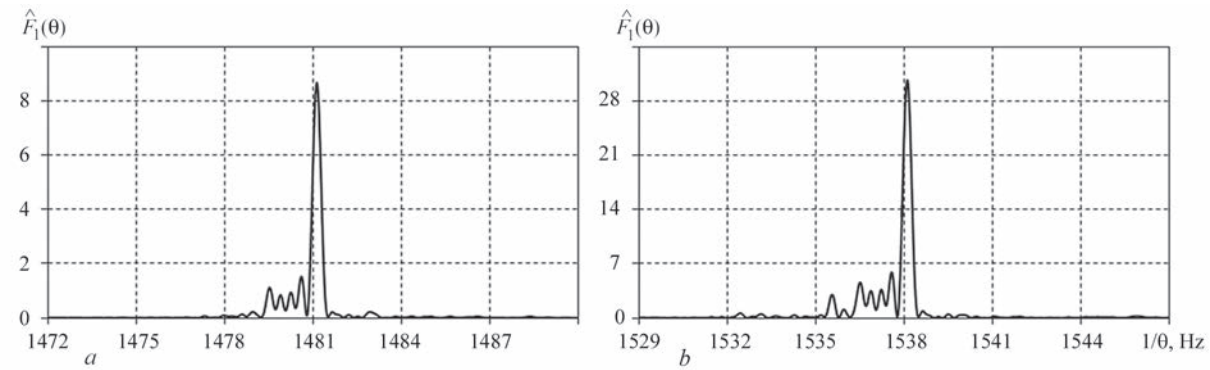

Figure 11. Dependencies of functional (9) on trial frequency in different frequency bands (*a*) and (*b*)

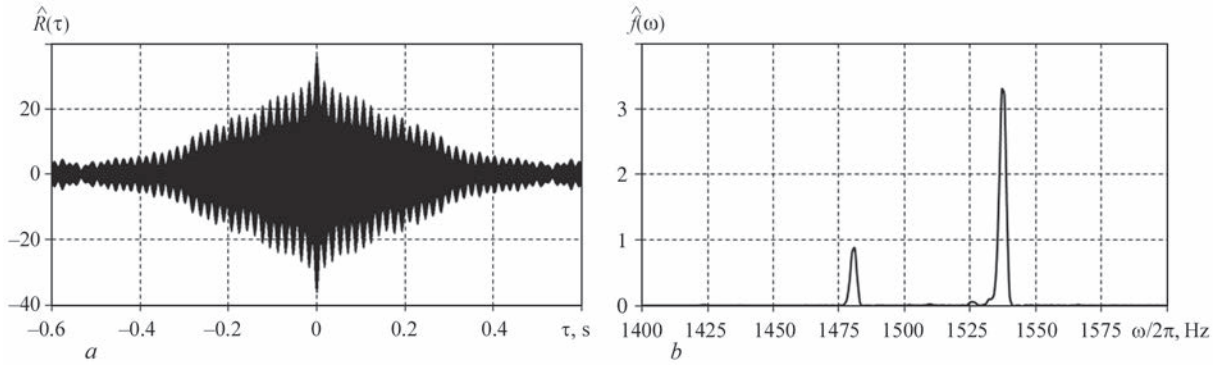

Figure 12. Correlation function (*a*) and spectral density (*b*) of the stochastic component of high-frequency signal

$$s_2(t)=\sum_{k=1}^{2}\left[\hat{a}_k\left(f_0^{(k)}\right)\cos 2\pi f_0^{(k)}t+\hat{b}_k\left(f_0^{(k)}\right)\sin 2\pi f_0^{(k)}t\right], \quad (12)$$

and will extract the stochastic component $\overset{\circ}{\xi}(nh)=\xi(nh)-s_2(t)$. Evaluation of its correlation function is slowly oscillationally vanishing to the level of low-power fluctuations and has group structure (Figure 12, *a*). Therefore, evaluation of spectral density, based on its correlation function, is peaked. Here, there exist two peaks, which are much larger than the others in magnitude at frequencies which practically coincide with those of the deterministic harmonics (Figure 12, *b*). Addition of oscillations with such close frequencies leads to the phenomenon of beating, where oscillations with frequency difference $f_1 - f_2$ are the frequencies, with which the main oscillation groups follow each other. Such beating is observed on the graphs of realization and evaluation of the correlation function.

In order to clarify whether these high-frequency oscillations are related to the low-frequency ones and in which way, we will search for hidden periodicities of the second order in the range, to which the rotor frequency belongs. For this purpose we will also use the least squares method, which in this case is reduced to analysis of frequency dependence of the functional:

$$\hat{F}_2(\theta)=\frac{1}{2K+1}\sum_{n=-K}^{K}R^2(nh,\theta), \quad (13)$$

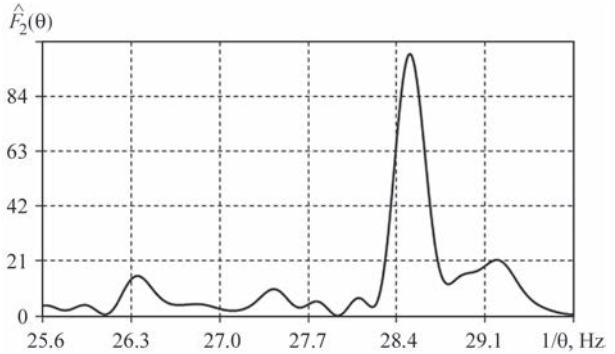

Figure 13. Dependence of quadratic functional (13) on trial frequency

where

$$\hat{R}(nh,\theta)=\sum_{k=1}^{L_2}\left[\hat{R}_k^c(\theta)\cos k\frac{2\pi}{\theta}nh+\hat{R}_k^s(\theta)\sin k\frac{2\pi}{\theta}nh\right], \quad (14)$$

$$\begin{Bmatrix}\hat{R}_k^c(\theta)\\ \hat{R}_k^s(\theta)\end{Bmatrix}=\frac{2}{2K+1}\sum_{n=-K}^{K}\overset{\circ}{\xi}^2(nh)\begin{Bmatrix}\cos k\frac{2\pi}{\theta}nh\\ \sin k\frac{2\pi}{\theta}nh\end{Bmatrix}, \quad (15)$$

Here, L_2 is the selected number of addends in the sum (14). For calculations it was assumed that $L_2 = 5$. Figure 13 presents the dependence of functional (13) on trial frequency $f = 1/\theta$. A pointed peak at frequency $\hat{f}_0 = 28.5$ Hz, which is close to that of rotor frequency, does not leave any doubt that the dispersion and correlation function of the stochastic component of vibrations are periodic function with engine rotor rotation period. As no other periodicities were revealed at analysis, presentations (8) in this case can be regarded as PNRP with period $P = P_1$.

Taking $\theta=\hat{P}=1/\hat{f}_0$, in (15), we will calculate Fourier coefficients of dispersion and its average value:

$$\hat{R}_0=\frac{1}{2K+1}\sum_{n=-K}^{K}\overset{\circ}{\xi}^2(nh).$$

Based on these values, we will formulate the following expression:

$$\hat{R}(t,\theta)=\hat{R}_0+\sum_{k=1}^{5}\left[\hat{R}_k^c(\theta)\cos k\frac{2\pi}{\hat{P}}t+\hat{R}_k^s(\theta)\sin k\frac{2\pi}{\hat{P}}t\right], \quad (16)$$

which, provided

$$h\le\frac{\hat{P}}{2L_2+1}$$

is the interpolation formula for dispersion. The graph of time dependence of dispersion (16) and its amplitude spectrum

$$\hat{V}\left(k\hat{f}_0\right)=\sqrt{\left[\hat{R}_k^c\left(\hat{P}\right)\right]^2+\left[\hat{R}_k^s\left(\hat{P}\right)\right]^2}$$

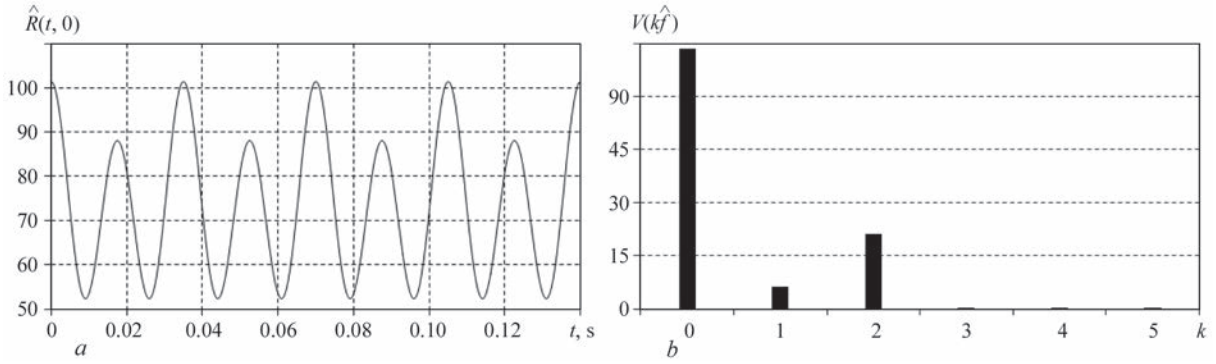

Figure 14. Dispersion (*a*) and its amplitude spectrum (*b*)

are shown in Figure 14. Only zero, first and second harmonics are significantly expressed in the spectrum.

Therefore, proceeding from the above results, we can assume that the time variability of dispersion is the result of modulation of the harmonics of low-frequency deterministic oscillations by stochastic high-frequency band oscillations, resulting from damage. The correlation function of such oscillations can be approximated by slowly vanishing oscillations with resonance frequency ν_0. The result of such a modulation in the frequency range is observed as narrowband peaks at frequencies $\nu_0 \pm k\hat{f}_0$ (Figure 11). Each high-frequency narrowband composition is a stationary random process; they, however, are cross-correlated. Here the cross-correlations of the components, the frequency distance between which is equal to $k\hat{f}_0$, determine the *k*-th component of dispersion. Based on these considerations, we can conclude that the second harmonics of dispersion is the result of modulation of the most powerful first harmonic of deterministic oscillations. Such a modulation leads to appearance of peak values in the frequency region at $\nu_0 - \hat{f}_0$ and $\nu_0 + \hat{f}_0$ frequencies. The cross-correlation function of these two stationary narrowband random processes, where the spectra are separated by $2\hat{f}_0$, determines the second harmonic of dispersion.

The detected modulations can be studied further on using Hilbert transform [18]. However, the above-established facts on the signal structure allow making a conclusion about the nature of the damage. An increased vibration level is not related to the probable defects in one of the bearing elements, but is attributable to wear of the bearing housing seat as a result of long-term operation of the mechanism. "Worn-out" hole in the housing causes sliding of the bearing outer ring, which, in its turn, excites powerful high-frequency oscillations.

CONCLUSIONS

The COMPACT-VIBRO system, developed at G.V. Karpenko Physico-Mechanical Institute of the NAS of Ukraine was used to select and analyze vibration signals from container handler mechanisms.

The methods for detection of hidden periodicities based on models in the form of PNRP and their generalizations were used to separate the deterministic and stochastic components of signals with higher RMS value level and to establish the characteristic features of each of them. The amplitude spectrum of deterministic components of vibrations was determined, and the deterministic and stochastic high-frequency modulation of their harmonics was detected. It is shown that such a modulation causes periodic nonstationarity of the second order with shaft rotor rotation period. The amplitude spectrum of time changes of signal dispersion was determined, and its connection with cross-correlations of the signal narrow-band high-frequency components was shown. The cause for the high vibration level, proceeding from the narrow band of dispersion spectrum and low values of its first harmonics, is bearing bushing damage propagation at the initial stage.

Calculated RMS values for Crane 1 and Crane 2 are within the normative range.

REFERENCES

1. Javorskyj, I.M. (2013) *Mathematical models and analysis of stochastic oscillations.* Lviv, PMI of NAS of Ukraine [in Ukrainian].
2. Javorskyj, I., Mykhailyshyn, V. (1996) Probabilistic models and statistical analysis of stochastic oscillations. *Pattern Recogn. Image. Anal.*, 6(**4**), 749–763.
3. Javorskyj, I., Yuzefovych, R., Kravets, I., Matsko, I. (2014) Methods of periodically correlated random processes and their generalizations. Cyclostationarity: Theory and Methods. Lecture Notes in Mechanical Engineering. Ed. by F. Chaari, J. Leskow, A. Sanches-Ramires. New York, Springer *Int. Publish. Switzerland*, 73–93.
4. Javorskyj, I., Dzeryn, O., Yuzefovych, R. (2019) Analysis of mean function discrete LSM-estimator for biperiodically nonstationary random signals. *Math. Model. Comput.*, 6(**1**), 44–57.
5. McCormick, A.C., Nandi, A.K. (1998) Cyclostationarity in rotating machine vibrations. *Mech. Syst. Signal Process.*, 12(**2**), 225–242.

6. Capdessus, C., Sidahmed, M., Lacoume, J.L. (2000) Cyclostationary processes: Application in gear fault early diagnostics. *Mech. Syst. Signal Process*., 14(**3**), 371–385.
7. Antoni, J., Bonnardot, F., Raad, A., El Badaoui, M. (2004) Cyclostationary modeling of rotating machine vibration signals. *Mech. Syst. Signal Process.*, **18**, 1285–1314.
8. Antoni, J. (2009) Cyclostationarity by examples. *Mech. Syst. Signal Process.*, **23**, 987–1036.
9. Randall, R.B., Antoni, J. (2011) Rolling element bearing diagnostics — A tutorial. *Mech. Syst. Signal Process.*, 25(**2**), 485–520.
10. Zimroz, R., Bartelmus, W. (2009) Gearbox condition estimation using cyclostationary properties of vibration signal. *Key Engineering Mater.*, 413(**1**), 471–478.
11. Hurd, H.L., Miamee, A. (2007) *Periodically correlated random sequences: Spectral theory and practice.* New York, Wiley.
12. Javorskyj, I., Kravets, I., Matsko, I., Yuzefovych, R. (2017) Periodically correlated random processes: Application in early diagnostics of mechanical systems. *Mech. Syst. Signal Process.*, **83**, 406–438.
13. Javorskyj, I., Matsko, I., Yuzefovych, R. et al. (2021) Methods of hidden periodicity discovering for gearbox fault detection. *Sensors*., **21**, 6138.
14. Javorskyj, I., Leśkow, J., Kravets, I. et al. (2011) Linear filtration methods for statistical analysis of periodically correlated random processes. Pt II: Harmonic series representation. *Signal Process.*, **91**, 2506–2519.
15. Yuzefovych, R., Javorskyj, I., Matsko, I. et al. (2020) Devices for detection of defects at early stages of their initiation at determination of technical condition of mechanisms. *Tekh. Diahnost. ta Neruiniv. Kontrol*, **4**, 8–16 [in Ukrainian]. DOI: https://doi.org/10.37434/tdnk2020.04.02.
16. Javorskyj, I., Yuzefovych, R., Lychak, O. et al. (2021) Methods and means of early vibrodiagnostics of bearing units of rotary mechanisms. *Tekh. Diahnost. ta Neruiniv. Kontrol*, **2**, 30–37 [in Ukrainian]. DOI: https://doi.org/10.37434/tdnk2021.02.04.
17. Javorskyj, I., Yuzefovych, R., Matsko, I., Zakrzewski, Z. (2021) The least square estimation of the basic frequency for periodically non-stationary random signals. *Digital Signal Process*., **116**, 103113. DOI: https://doi.org/10.1016/j.dsp.2021.103333.
18. Javorskyj, I., Yuzefovych, R., Matsko, I., Kurapov, P. (2021) Hilbert transform of a periodically non-stationary random signal: Low-frequency modulation. *Digital Signal Process.*, **116**, 103113. DOI: https://doi.org/10.1016/j.dsp.2021.103113.

ORCID

I.M. Javorskyi: 0000-0003-0243-6652,
R.M. Yuzefovych: 0000-0001-5546-453X,
O.V. Lychak: 0000-0001-5559-1969

CONFLICT OF INTEREST

The Authors declare no conflict of interest

CORRESPONDING AUTHOR

R.M. Yuzefovych
Karpenko Physico-Mechanical Institute
of the NASU
5 Naukova Str., 79060, Lviv, Ukraine
E-mail: roman.yuzefovych@gmail.com

SUGGESTED CITATION

I.M. Javorskyi, R.M. Yuzefovych, O.V. Lychak, P.O. Semenov (2022) Methods and means of early vibration diagnostics of rotating components of mechanisms of quay container handlers. *The Paton Welding J.*, **1**, 48–58.

JOURNAL HOME PAGE

https://pwj.com.ua/en

Received: 07.12.2021
Accepted: 07.02.2022